

## Quasielastic ( $p,n$ ) Angular Distributions\*

J. D. ANDERSON, C. WONG, J. W. McCLURE, AND B. D. WALKER  
*Lawrence Radiation Laboratory, University of California, Livermore, California*  
 (Received 22 May 1964)

Previously reported neutron spectra resulting from the ( $p,n$ ) reaction all showed one strong neutron group at an energy corresponding in excitation in the final nucleus to the isobaric counterpart (analog state) of the target ground state, i.e., the  $Q$  value for the reaction is the usual Coulomb displacement energy. Using time-of-flight techniques and the higher proton energies available from the 90-in. cyclotron after recent modifications, we have measured the angular distributions of the neutrons from the isobaric ( $p,n$ ) reaction for 18.5-MeV protons on 19 targets between Be<sup>9</sup> and Nb<sup>93</sup>. The optical model, with the inclusion of the isospin term as suggested by Lane, is capable of explaining the diffractive nature of the ( $p,n$ ) angular distributions and the absolute magnitude of the cross sections. The strength of the isospin potential ( $V_1$ ) obtained from the quasielastic ( $p,n$ ) reaction ( $V_1 \approx 70$ –90 MeV) is in agreement with the magnitude calculated from the proton potential anomaly ( $V_1 \approx 100$  MeV).

### I. INTRODUCTION

RECENT experimental work<sup>1-4</sup> has shown that the ( $p,n$ ) reaction on medium- $A$  nuclei excites relatively strongly a state in the residual nucleus which is the isobaric analog of the target ground state. Lane<sup>5</sup> has pointed out that the optical-model potential for nucleons should depend upon isotopic spin, containing a term proportional to  $(\mathbf{t} \cdot \mathbf{T})$ , where  $\mathbf{t}$  is the isotopic spin of the incident nucleon and  $\mathbf{T}$  is the isotopic spin of the target nucleus. This term then can induce a ( $p,n$ ) reaction in which the target is transformed into its isobaric analog. It has also been pointed out that the

quasielastic ( $p,n$ ) reaction is sensitive to the strength<sup>5-7</sup> and form<sup>8,9</sup> of the  $(\mathbf{t} \cdot \mathbf{T})$  potential.

Using time-of-flight techniques<sup>10</sup> and the higher energy protons available from the 90-in. cyclotron after recent modifications, we have measured the angular distributions of the quasielastic ( $p,n$ ) reaction for 18.5-MeV protons on Be, B<sup>11</sup>, N<sup>15</sup>, Ti, V, Cr, Mn, Fe, Co, Ni, Cu<sup>63</sup>, Cu<sup>65</sup>, and Nb in approximately 15° steps between 3 and 153°. Angular distributions were also obtained for C<sup>13</sup>, Sc, Y, and Zr in approximately 30° steps and partial angular distributions were measured for Se and Sr. At a proton bombarding energy of 17 MeV, angular distributions were measured for B<sup>11</sup>, Ti, V, Fe, and for the first excited isobaric states of B (C<sup>11</sup>) and Fe (Co<sup>56</sup>).

### II. EXPERIMENTAL METHOD

#### A. Geometry

In order to facilitate the measurement of the quasielastic ( $p,n$ ) reaction angular distribution, considerable modification of the Livermore time-of-flight instrumentation has been necessary.<sup>11</sup> In particular these modifications include the construction of 10-m flight paths at 3, 30, 60, 90, 120, and 135° and the installation of an additional bending magnet and auxiliary equipment to double-bend the proton beam so that its incident angle at the target is 18° to the normal beam line, thus doubling the number of angles for which measurements can be made (Fig. 1). The 10-m flight paths are collimated so that the detectors view directly only a few inches around the target area, thus reducing background from the "beam catcher" and sweeping slits.

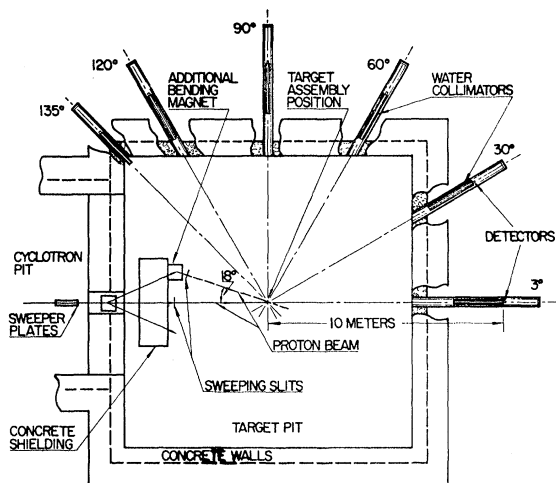


FIG. 1. Schematic diagram of the experimental geometry.

\* The subject of this paper was discussed in part by the first-named author at the Symposium on Nuclear Spectroscopy with Direct Reactions, Chicago, March 1964.

<sup>1</sup> J. D. Anderson and C. Wong, *Phys. Rev. Letters* **7**, 250 (1961).

<sup>2</sup> J. D. Anderson, C. Wong, and J. W. McClure, *Phys. Rev.* **126**, 2170 (1962).

<sup>3</sup> J. D. Anderson, C. Wong, and J. W. McClure, *Phys. Rev.* **129**, 2718 (1963).

<sup>4</sup> C. J. Batty, G. H. Stafford, and R. S. Gilmore, *Phys. Letters* **6**, 292 (1963).

<sup>5</sup> A. M. Lane, *Phys. Rev. Letters* **8**, 171 (1962); *Nucl. Phys.* **35**, 676 (1962).

<sup>6</sup> P. E. Hodgson and J. R. Rook, *Nucl. Phys.* **37**, 632 (1962).

<sup>7</sup> R. M. Drisko, R. H. Bassel, and G. R. Satchler, *Phys. Letters* **2**, 318 (1962).

<sup>8</sup> J. B. French and M. H. Macfarlane, *Phys. Letters* **2**, 255 (1962).

<sup>9</sup> T. Terasawa and G. R. Satchler, *Phys. Letters* **7**, 265 (1963).

<sup>10</sup> J. D. Anderson and C. Wong, *Nucl. Instr. Methods* **15**, 178 (1962).

<sup>11</sup> B. D. Walker, J. D. Anderson, J. W. McClure, and C. Wong, *Nucl. Instr. Methods* (to be published); Lawrence Radiation Laboratory, Livermore, Report No. UCRL-7612, 1963 (unpublished).

### B. Targets

The targets used varied in thickness from 100 to 300 keV. The Be, V, Ni, Cu, and Nb were obtained commercially as foils. The Ti, Fe, Co, and Cu were evaporated and lifted as free films, while the Cr and Mn were of sandwich construction, i.e., electrodeposited on both sides of a  $\frac{1}{10}$ -mil gold foil. The B, Sc, Se, Sr, Y, and Zr were made as colloidal suspensions with  $\frac{1}{2}$ -mil Mylar backing. Because of the nonuniformity of these colloidal targets, there is at least a 20% uncertainty in the target thickness. The gas targets  $C^{13}$  and  $N^{15}$  were also self-supporting, i.e., the gas was contained in a low-mass cell with a  $\frac{1}{4}$ -mil tantalum entrance and exit foil.

### C. Electronics

A schematic diagram of the time-of-flight electronics is shown in Fig. 2. The slow-fast system is conventional and has been described in a previous paper.<sup>10</sup> The only additional complexity is that required for the simul-

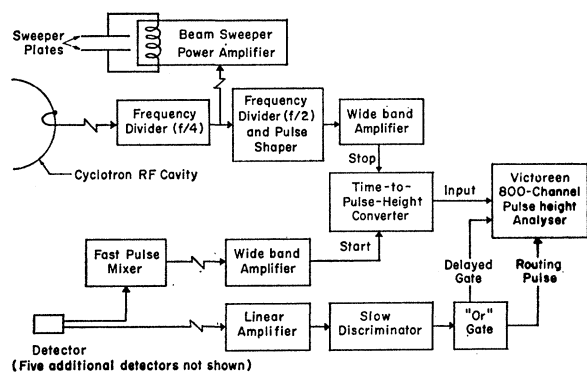


FIG. 2. Schematic diagram of the time-of-flight electronics.

taneous data accumulation for the six detectors. The 2-in.-diam by 2-in.-long plastic scintillators were used in place of the standard 1-in. by 1-in. plastic to increase the detector efficiency and thus increase the count rate.

The new detectors were intercalibrated using 14-MeV neutrons and were calibrated with respect to a standard 1-in. by 1-in. plastic.<sup>12</sup> These measurements were in agreement with the calculated efficiencies.<sup>13</sup> It is inferred then that the absolute error in cross sections obtained with this system is less than 10% due to detector efficiency uncertainties.

### III. RESULTS

The time-of-flight spectra resulting from 17-MeV proton bombardment of  $B^{11}$  are shown in Fig. 3. The effect of center-of-mass motion on the laboratory neutron energy is seen quite clearly. These spectra are

<sup>12</sup> M. D. Goldberg, J. D. Anderson, J. P. Stoering, and C. Wong, Phys. Rev. **122**, 1510 (1961).

<sup>13</sup> A. Elwyn, J. V. Kane, S. Ofer, and D. H. Wilkinson, Phys. Rev. **116**, 1490 (1959).

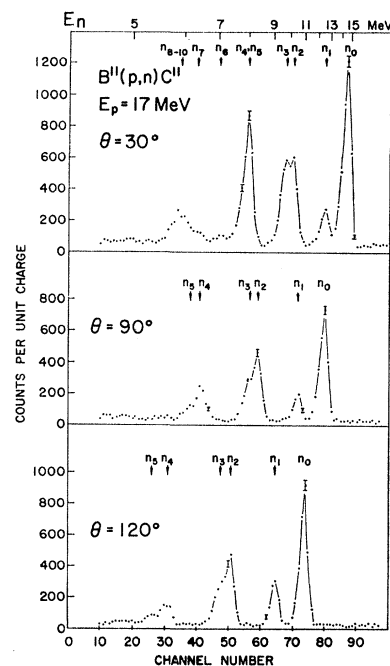


FIG. 3. Time-of-flight spectrum from 17-MeV proton bombardment of  $B^{11}$ . Increasing time of flight is toward the left while increasing neutron energies are toward the right. The neutron groups corresponding to the ground and excited states of  $C^{11}$  are indicated.

not, however, characteristic of the ( $p, n$ ) reaction on medium- $A$  nuclei. In Fig. 4 the spectrum at  $60^\circ$  is shown for proton bombardment of Fe. The neutron groups have been previously identified as follows<sup>3</sup>: (1) configuration state (A), (2) isobaric state ( $n_0$ ), and (3) excited isobaric states ( $n_1, n_2, n_3,$  and  $n_4$ ).

Angular distribution data (Figs. 5–8) were taken in two steps: 3, 30, 60, 90, 120, and  $135^\circ$  were obtained simultaneously, and then the proton beam was doubly bent to strike the target at  $18^\circ$  to the normal beam line and the 18, 48, 78, 108, 138, and  $153^\circ$  data were obtained. The measured cross sections were corrected for dead time, typically a 10% correction. No correction was necessary for neutron attenuation in the target assembly. The relative angular distributions for the

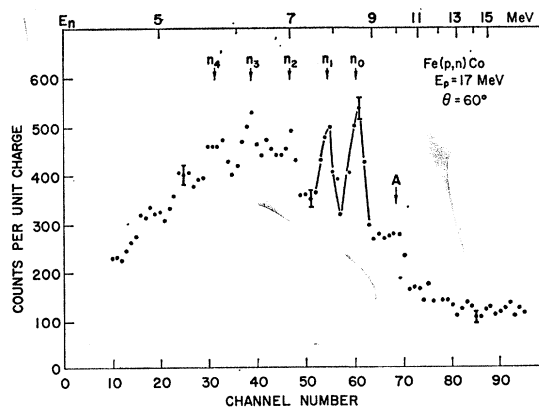


FIG. 4. Time-of-flight spectrum from 17-MeV proton bombardment of Fe. The peaks have previously been identified as, (A) configuration state, ( $n_0$ ) isobaric analog of the target ground state, and ( $n_1$ – $n_4$ ) excited isobaric states (see Ref. 3).

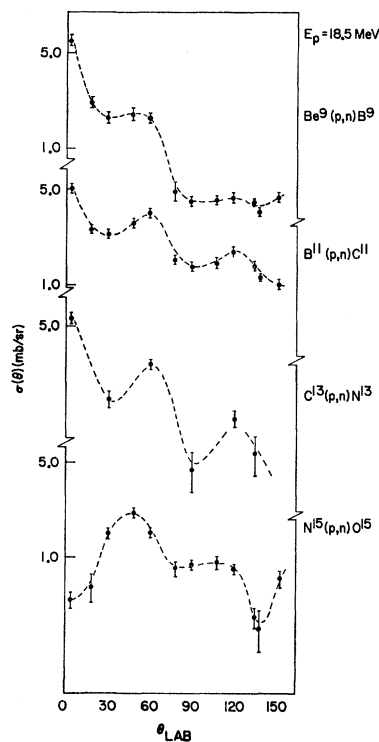


FIG. 5. Angular distributions of the neutrons from the  $(p,n)$  reaction on light nuclei for an incident proton energy of 18.5 MeV.

light elements were corrected for the energy sensitivity of the detector, i.e., for 18-MeV protons on Be the neutron energy varies from 10.6 MeV at  $150^\circ$  to 16.3 MeV at  $0^\circ$ .

The errors are computed from the statistical errors and the errors due to uncertainties in line shape using the usual error propagation formula. As shown in Fig. 4, one of the largest uncertainties in data analysis is associated with the subtraction of background due to other direct processes and continuum neutrons such that it is necessary to use a line shape in order to extract the angular distribution data. This produces no appreciable error where the neutron group is prominent (near  $0^\circ$ ) but accounts for most of the error near minima in the angular distributions.

The angular distributions of neutrons from the mirror nuclei (Fig. 5) are quite similar with the exception of  $N^{15}$ . The forward peaking of the cross sections seen here has previously been noted at lower bombarding energies.<sup>14</sup> Since the integrated  $N^{15}$  cross section (12 mb) is actually larger than the Be cross section (11 mb) it is suggested that the inversion in shape of the  $N^{15}$  cross section does not imply a different reaction mechanism but is rather an interference phenomenon. The  $A$  dependence of the mirror nuclei zero-degree cross sections are then characterized by large fluctuations (a factor of 10) while the integrated cross sections vary less than a factor of 2.

In Fig. 6 the medium- $A$  nuclei (40–60) data are

<sup>14</sup> C. Wong, J. D. Anderson, S. D. Bloom, J. W. McClure, and B. D. Walker, Phys. Rev. 123, 598 (1961).

presented. Here one notes a characteristic minimum between  $30$  and  $45^\circ$ , and a second pronounced minimum at about  $140^\circ$ . There is also some evidence for an additional minimum at  $100^\circ$  (see Cr, Fig. 6). In addition to the pronounced forward peaking of the cross section there is evidence for backward peaking ( $\theta > 150^\circ$ ). Again we note large fluctuations in the differential cross sections, e.g., the variation for Sc is a factor of 5 while for cobalt the variation is almost two orders of magnitude. However, even though there are large fluctuations in the shape of the distributions, the integrated cross sections vary by only a factor of 2, e.g., for Sc  $\sigma = 5$  mb and for Co  $\sigma = 4$  mb. One should also note that there are no systematic differences between the odd-even and even-even angular distributions.

As one proceeds to heavier nuclei (Fig. 7), the first minimum near  $40^\circ$  which was so prominent for Ti and V gradually disappears. For Zr and Nb the second prominent minimum which was at  $140^\circ$  for V has now moved in to  $120^\circ$ . Again one sees that the general features of the differential cross sections change more radically as a function of  $A$  than do the integrated cross sections. One also notes relatively little difference in shape between the angular distributions for the predominantly even-even isotopes of Zr and the odd-even nucleus Nb.

In Fig. 8, the data for 17-MeV incident protons are presented. One notes that although the  $3^\circ$  cross section for  $B^{11}$  has changed almost a factor of 2 the other differential cross sections are the same and thus the integrated cross section is virtually unchanged. The 17-MeV data are in general unchanged as compared to the 18.5-MeV data. In addition to the ground state,

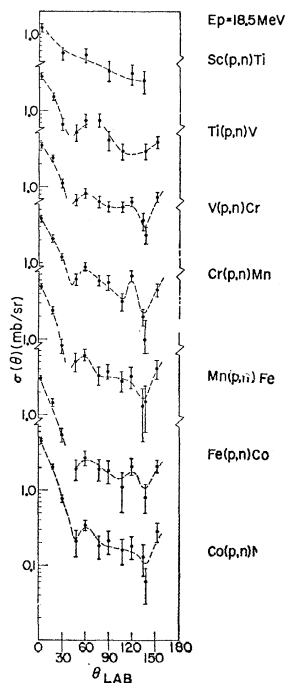


FIG. 6. Angular distributions of the neutrons from the isobaric state  $(p,n)$  reaction on the medium- $A$  nuclei between  $Sc^{45}$  and  $Co^{59}$  for an incident proton energy of 18.5 MeV.

the first excited-state angular distributions were also obtained for  $B^{11}$  and  $Fe^{56}$ . It is an interesting feature of these measurements that the ratio of ground state to first excited state is approximately the same for the two nuclei, i.e., for  $B^{11}$  the ratio is about 4 while for Fe it is roughly 2.

#### IV. THEORY

##### A. Introduction

When optical-model potentials are used to compute elastic scattering of protons and neutrons or sequences of bound levels of neutrons and protons, the proton potential must be made deeper than the neutron potential to obtain proper agreement with experiment. This difference in the well depths, the so-called proton potential anomaly, has been the subject of study for a large number of investigators during recent years.<sup>15,16</sup> This potential is generally written

$$V_{p,n} = V_0 \pm [(N-Z)/4A]V_1, \quad (1)$$

where  $V_p$  represents the average potential acting on a proton and  $V_n$  that acting on a neutron; the upper sign is for neutrons and the lower one for protons.

Lane<sup>5</sup> noted that an isotopic-spin-dependent potential arises straightforwardly in a potential calculation taken as a sum of two-body forces with Heisenberg components and averaged over a Fermi gas. He proposed the optical potential should be of the form

$$V = V_0 + (\mathbf{t} \cdot \mathbf{T})V_1/A, \quad (2)$$

where  $V_0$  is the ordinary optical potential,  $\mathbf{t}$  is the

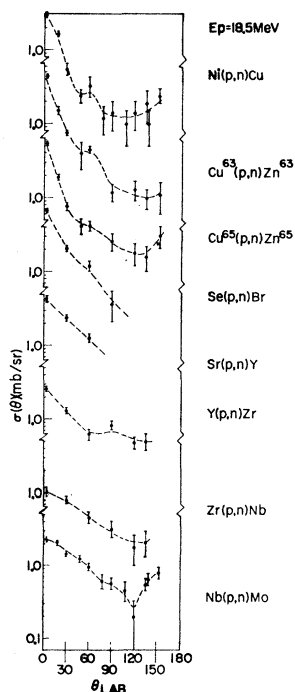


FIG. 7. Angular distributions of the neutrons from the isobaric state ( $p, n$ ) reaction on nuclei between Ni and Nb<sup>98</sup> for an incident proton energy of 18.5 MeV.

<sup>15</sup> A. E. S. Green and P. C. Sood, Phys. Rev. **111**, 1147 (1958).

<sup>16</sup> P. C. Sood, Nucl. Phys. **37**, 624 (1962).

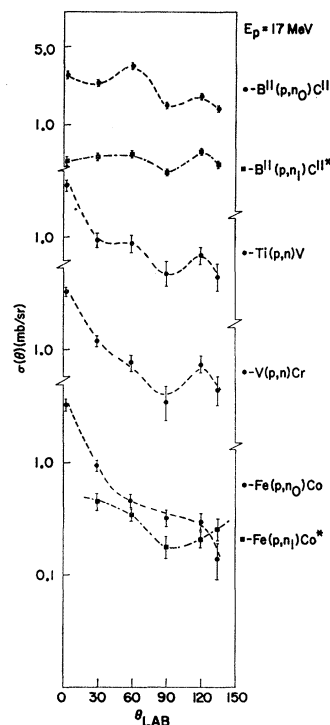


FIG. 8. Angular distributions of the neutrons from the isobaric state ( $p, n$ ) reaction on selected nuclei for an incident proton energy of 17 MeV. The angular distributions of the neutrons from the first excited isobaric states resulting from the ( $p, n$ ) reaction on  $B^{11}$  and  $Fe^{56}$  are also shown.

isotopic spin of the incident particle, and  $\mathbf{T}$  is the isotopic spin of the target nucleus  $A$ . In addition to reproducing the proton potential anomaly [Eq. (1)] the isospin term ( $t_+ T_-$ ) acting on an incident proton can convert it into a neutron, and turn the target into the corresponding isobaric state thus resulting in a quasielastic ( $p, n$ ) reaction.

Several authors<sup>5-9</sup> have pointed out that the quasielastic ( $p, n$ ) reaction is sensitive to the strength of the isospin potential ( $V_1$ ) and to its radial dependence. It has also been noted that  $V_1$  itself may be angular momentum dependent.<sup>6-8</sup> However, in order to evaluate the ( $p, n$ ) cross section some approximations must be made at present in solving the coupled Schrödinger equations which result from Eq. (2).

##### B. Plane-Wave Born Approximation

In order to obtain a rough estimate of the cross section which may indicate trends with mass number and energy we use Lane's<sup>5</sup> procedure as follows. The cross section for the ( $p, n$ ) process is

$$\sigma_{pn}(\theta) = (k_n/k_p) |f_{pn}(\theta)|^2, \quad (3)$$

where  $k_n$  and  $k_p$  are the neutron and proton wave numbers and where

$$f_{pn}(\theta) = \frac{M}{2\pi\hbar^2} \left\langle g_{n0}^{\theta-} \left| \frac{1}{2A} (2T_0)^{1/2} V_1 \right| g_p \right\rangle. \quad (4)$$

Here  $g_{n0}^{\theta-}$  and  $g_p$  are wave functions with unit amplitude (plane waves) in the final and initial directions

TABLE I. Optical-model parameters used in computing the mirror nuclei ( $p,n$ ) angular distributions. The notation is that of Ref. 20. The surface-centered absorption is of the Gaussian form.

Element	$V$ (MeV)	$W$ (MeV)	$V_1$ (MeV)	$r_0$ (F)	$a$ (F)	$b$ (F)	Comments
Be	40.7	22.2	-5.0	1.4	0.62	0.39	Lutz (Ref. 20)
B	42.4	9.4	-5.0	1.35	0.55	0.75	Lutz (Ref. 20)
C	50.5	6.8	-5.0	1.23	0.51	0.81	Lutz (Ref. 20)
C	51.2	17.7	-5.5	1.25	0.37	0.25	Nodvik (Ref. 18), $E_p=17.4$ MeV
C	55.0	11.5	-2.7	1.20	0.50	0.50	Nodvik (Ref. 18), $E_p=18.4$ MeV
N	48.5	7.0	-5.0	1.20	0.71	1.00	Lutz (Ref. 20)
N	47.5	28.0	-12.3	1.25	0.60	0.20	Duke (Ref. 19), $E_p=17.0$ MeV
N	46.4	4.8	-2.3	1.25	0.57	1.20	Duke (Ref. 19), $E_p=18.4$ MeV

(see Ref. 5),  $T_0$  is the isotopic spin of the target nucleus, and  $V_1$  is the magnitude of the isospin potential. With the assumption that the  $g$  functions become negligible through absorption in the nuclear interior and are approximated by plane waves in the outer skin of the nucleus of depth  $\Delta R$ , then for small angles

$$\sigma_{pn}(\theta) = \left( \frac{V_1 r_0^2 \Delta R}{42} \right)^2 \frac{N-Z}{A^{3/2}} \left( \frac{k_n}{k_p} \right) \left( \frac{\sin qR}{qR} \right)^2, \quad (5)$$

where  $q = |\mathbf{k}_p - \mathbf{k}_n|$  and  $R = r_0 A^{1/3}$ . The angular distribution for small angles is given by the  $[\sin qR/qR]^2$  term. The energy dependence is contained in the two terms  $(k_n/k_p)$  and  $[\sin qR/qR]^2$  while the variation of the zero-degree cross section with  $A$  includes contributions from all terms. It is not too surprising because of the crude assumptions that this expression gives an adequate fit to the small-angle scattering for only a few

nuclei. A few of the best fits are shown in Fig. 9. From these nuclei, assuming  $r_0 = 1.2$  F and  $\Delta R = 1$  F, one obtains a very reasonable value of  $V_1 \approx 50$  MeV in the region of the nuclear surface. A change of  $r_0$  from 1.2 to 1.4 F does not seriously alter these results in that  $[\sin qR/qR]^2$  is also a function of  $r_0$  and this tends to cancel the  $r_0^2$  term which multiplies  $V_1$ . Although these results are encouraging, Eq. (5) does not generally reproduce the  $A$ , energy, or angular dependence of the ( $p,n$ ) measurements.

### C. Optical-Model Calculations Neglecting the Coulomb Potential

If the incident energy is high enough for Coulomb effects to be small, this includes both the distortion of the proton wave and the fact that the neutron energy is less than the proton energy by the Coulomb displacement energy; then by neglecting the Coulomb terms the coupled equations resulting from the inclusion of the isospin potential  $(\mathbf{t} \cdot \mathbf{T})V_1$  can be solved to yield<sup>5,6</sup>

$$\sigma_{pn}(\theta) = [2T_0/(2T_0+1)^2] |f_{T_0+\frac{1}{2}}(\theta) - f_{T_0-\frac{1}{2}}(\theta)|^2, \quad (6)$$

where the  $f(\theta)$ 's are the scattering amplitudes corresponding to the two values of the total isotopic spin. Assuming the form factor of the isospin term is the same as that of the real part of the optical potential, Hodgson and Rook<sup>6</sup> noted the sensitivity of the ( $p,n$ ) cross section to this potential. However, with the limited data available (a partial angular distribution for 12-MeV protons on vanadium) no accurate estimate could be made of the magnitude of  $V_1$  or its form factor.

The optical-model code `LOKI`,<sup>17</sup> including a spin orbit term, has been modified to allow calculations similar to those of Hodgson and Rook.<sup>6</sup> Several sets of parameters used in fitting elastic scattering data were tried; however, no extensive parameter search was carried out. The calculated ( $p,n$ ) cross sections scale quite accurately as  $V_1^2$ .

Considering the uncertainties in application of the optical model neglecting Coulomb effects, it was thought more interesting to note the results of various sets of parameters which have evolved from elastic scattering

<sup>17</sup> We are indebted to Dr. E. Schwarcz for modifying the optical-model code to include the isospin potential.

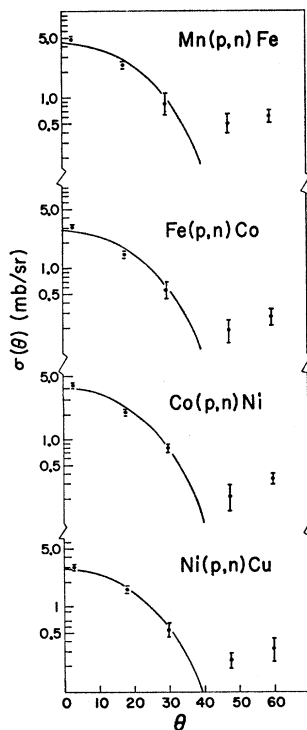


FIG. 9. The results of plane-wave-surface approximation calculations are compared with the experimental data for small angles.

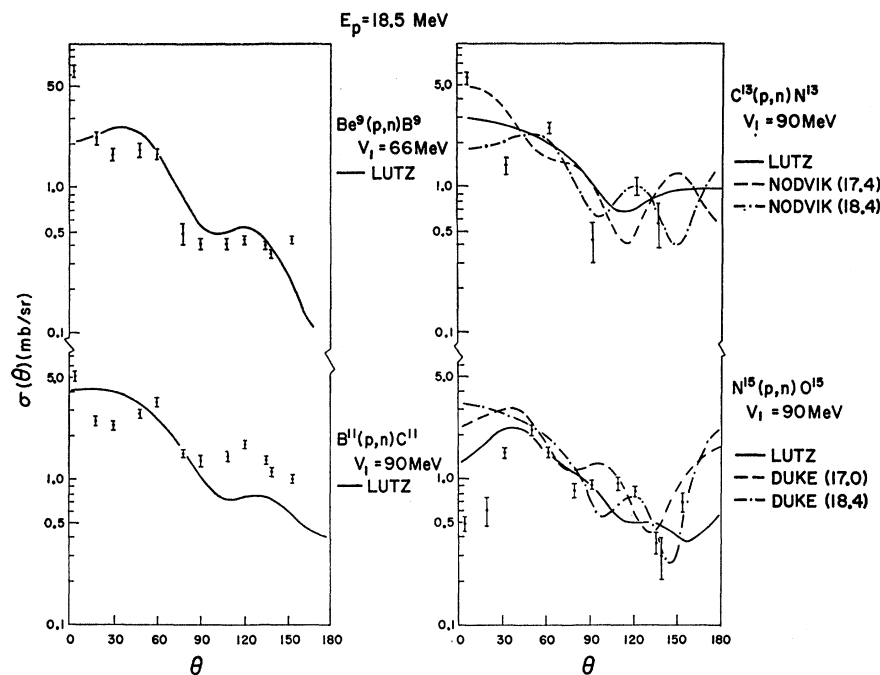


FIG. 10. Optical-model calculations neglecting Coulomb effects are shown for the true mirror nuclei together with the experimental data. The optical model parameters used are listed in Table I.

data rather than to try to obtain a totally new consistent set of parameters.

The results of these calculations follow.

### 1. Mirror Nuclei

For  $C^{12}$  and  $O^{16}$ , rather complete investigations have been carried out in determining the optical-model parameters from proton elastic scattering.<sup>18,19</sup> In addition Lutz *et al.*<sup>20</sup> have investigated the optical parameters for light nuclei in fitting the elastic scattering of 14-MeV neutrons. The predicted angular distributions resulting from the inclusion of the isospin potential and these rather specialized potential parameters are displayed in Fig. 10 along with the measurements. In Table I the parameters corresponding to the various curves are listed.

It is interesting to note that although none of the calculations yield a particularly good fit to the data, the magnitude of the predicted cross section is approximately correct for a value of  $V_1$  of 90 MeV except for Be where a value of 60 MeV gives an appreciably better fit to the data. It is also clear that the optical calculations are capable of reproducing the prominent features of the angular distributions, although those employed here do not reproduce all the maxima and minima found in the data. It is concluded that the true mirror nuclei data can be adequately described with the optical model although the agreement is not overly impressive.

<sup>18</sup> J. S. Nodvik, C. B. Duke, and M. A. Melkanoff, *Phys. Rev.* **125**, 975 (1962).

<sup>19</sup> C. B. Duke, *Phys. Rev.* **129**, 681 (1963).

<sup>20</sup> H. F. Lutz, J. B. Mason, and M. D. Karvelis, *Nucl. Phys.* **47**, 521 (1963).

### 2. Nonmirror Nuclei

The basic assumption that the Coulomb effects are small is not valid in this case. In trying to account at least partially for the Coulomb effects, calculations were made using the average nucleon energy, i.e., the incident energy used in the optical model is assumed to vary as  $(E_p - \frac{1}{2}\Delta E_c)$ , where  $\Delta E_c$  is the Coulomb displacement energy. This energy adjustment has previously proved quite useful in comparing true mirror nuclei data.<sup>14</sup>

In Fig. 11 the results of optical-model calculations using both volume and surface absorption are displayed. The pertinent parameters<sup>21,22</sup> are listed in Table II. A rather thorough discussion of the various parameters may be found in a recent article by Perey.<sup>22</sup>

It is immediately obvious that although there is excellent agreement with the Cr data and fair agreement with the Nb, the other data do not agree well with the model. Again as in the light nuclei the optical model is able to predict reasonably well the magnitude of the cross sections but, in general, does not fit the detailed shape of the angular distribution. The over-all agreement using volume absorption is slightly better than that for the surface-centered absorption.

With the assumption that the isospin potential has the same form factor as the real potential and volume absorption one concludes that  $V_1$  varies from 60 to 90

<sup>21</sup> M. Gursky and C. E. Porter, in *Proceedings of the International Conference on the Nuclear Optical Model, Tallahassee, Florida 1960* (Florida State University Research Council, Tallahassee, Florida, 1959), p. 85.

<sup>22</sup> F. G. Perey, *Phys. Rev.* **131**, 745 (1963).

TABLE II. Optical-model parameters used in computing the nonmirror nuclei ( $p,n$ ) angular distributions. The notation is that of Ref. 20.

Absorption	$V$ (MeV)	$W$ (MeV)	$V_s$ (MeV)	$r_0$ (F)	$a$ (F)	$b$ (F)	Comments
Surface-centered, of Gaussian form	48.0	11.5	-7.5	1.25	0.65	0.98	Ref. 22
Volume	55.0	7.0	-6.7	1.22	0.55	0.55	Ref. 21

MeV. Where the over-all fit to the data is good, such as for Cr, the value obtained for  $V_1$  is  $90 \pm 10$  MeV.

In general, the optical model including the isospin potential, but neglecting Coulomb effects, is capable of predicting the order of magnitude of the ( $p,n$ ) cross section, the diffraction character of the angular distribution, and the rapid variation of angular shape as a function of the atomic weight of the bombarded nucleus. These calculations do not, however, give detailed agreement with the data. In the light nuclei this disagreement may be due to the rapid fluctuation of optical parameters with energy, and perhaps the shell-model formalism of Bloom *et al.*<sup>23</sup> may be a more valid description. With medium- $A$  nuclei the assumption that the Coulomb effects are negligible is of course no longer valid since the incident energy is not large compared to the Coulomb displacement energy.

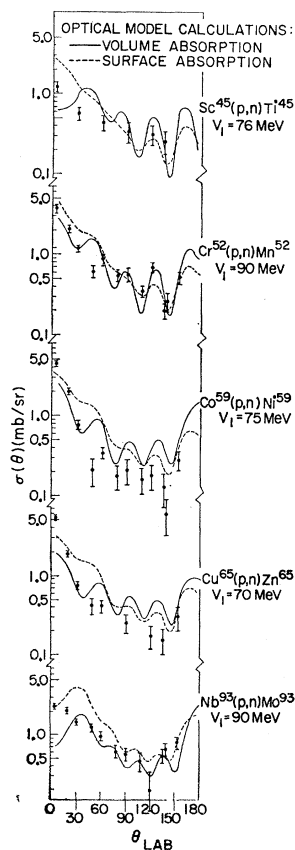


FIG. 11. Optical-model calculations neglecting Coulomb effects are shown for medium- $A$  nuclei together with the experimental data. The optical-model parameters for surface absorption are those of Perey while the volume absorption parameters are similar to those of Gursky and Porter (see Table II).

<sup>23</sup> S. D. Bloom, N. K. Glendenning, and S. A. Moszkowski, Phys. Rev. Letters 3, 98 (1959).

## D. Distorted-Wave Born Approximation (DWBA)

Drisko *et al.*<sup>7</sup> have studied the effects of the isospin term in the optical potential in distorted-wave Born approximation (DWBA).<sup>24</sup> Using the DWBA they were able to account for the Coulomb distortion of the incident proton and for the fact that the neutron energy may be significantly less than the incident proton energy, differing by the Coulomb displacement energy.

In Fig. 12, the optical-model calculations neglecting Coulomb effects [Eq. (6)] and with a volume isospin potential and surface absorption are compared with the corresponding DWBA calculations. As expected, in the light elements there is little difference between the two calculations.<sup>25,26</sup> Even for nuclei with  $A$  between 40

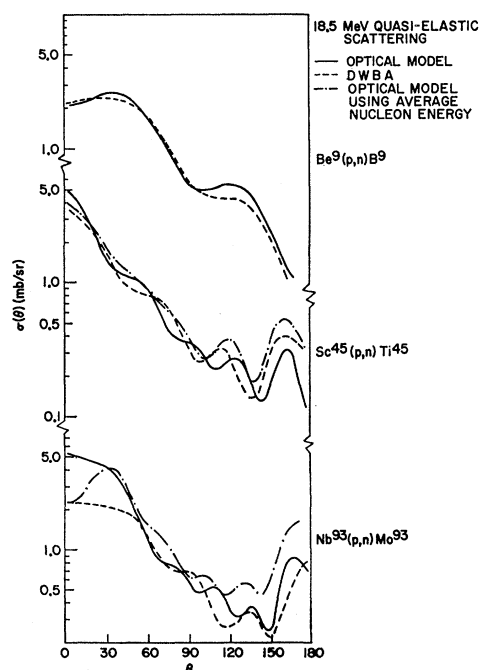


FIG. 12. The quasielastic ( $p,n$ ) optical-model calculations neglecting Coulomb effects are compared to the results obtained using the DWBA which includes the Coulomb effects. The effect of using the average nucleon energy ( $E = E_p - \frac{1}{2}\Delta E_c$ ) rather than the incident proton energy ( $E_p$ ) in the optical-model calculations is also shown.

<sup>24</sup> G. R. Satchler, R. M. Drisko, and R. H. Bassel, Phys. Rev. (to be published).

<sup>25</sup> Previously reported differences (Ref. 26) between these two calculations for the case of  $N^{16}(p,n)O^{16}$  were at least in part due to an error in the optical-model code LOKI.

<sup>26</sup> Luisa F. Hansen and Marion L. Stelts, Phys. Rev. 132, 1123 (1963).

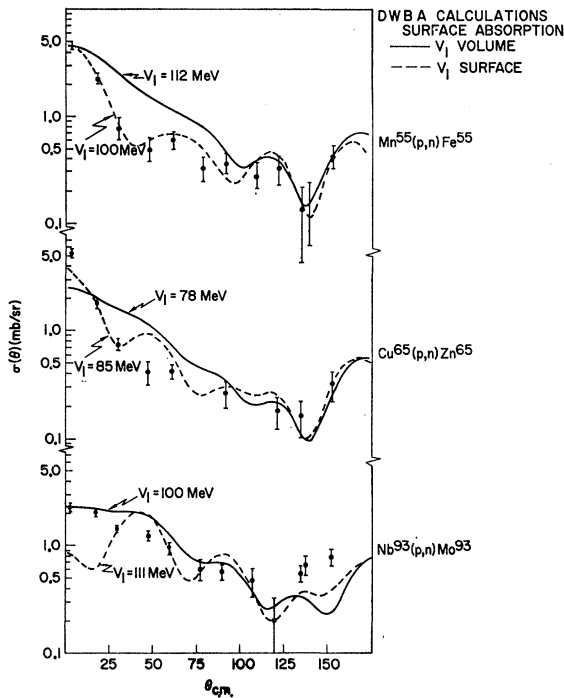


FIG. 13. The DWBA calculations of Satchler are shown both for a volume and a surface-centered isospin potential together with the experimental data.

and 60 the agreement between calculations is sufficiently good so that values of  $V_1$  inferred from the optical model (neglecting Coulomb) are probably reliable. It is clear, however, that for  $A > 60$  the neglect of Coulomb effects renders the optical calculations unreliable and one must employ the DWBA in order to obtain a reliable estimate of the isospin potential.

In addition to producing reliable estimates of the strength of the isospin potential the DWBA calculations, described in detail elsewhere,<sup>24</sup> using a surface-centered isospin potential yields a significantly better fit to the medium- $A$  nuclei than the volume isospin term. The calculations for a few nuclei are shown in Fig. 13. The results of Satchler *et al.*<sup>24</sup> would seem to indicate that there is some surface peaking of the isospin potential.

## V. CONCLUSIONS

It is clear that the inclusion of the isospin term in the optical potential is capable of explaining the diffractive nature of the ( $p, n$ ) angular distribution and the absolute

magnitude of the cross section. The results of these calculations are summarized as follows:

(1) The optical model neglecting Coulomb and the DWBA yield comparable results when the Coulomb displacement energy is small compared to the incident proton energy, i.e., for  $\Delta E_c < E_p/2$ .

(2) Assuming the isospin potential has the same form factor as the real potential assuming volume absorption, and neglecting Coulomb effects, one obtains values for  $V_1$  which vary, as a function of  $A$ , from 70 to 90 MeV.

(3) The value for  $V_1$  (70–90 MeV) inferred from the ( $p, n$ ) cross sections is in good agreement with the determination of the proton potential anomaly<sup>16</sup> ( $\sim 100$  MeV). It is seen then that the isospin term in the optical potential proposed by Lane<sup>5</sup> accounts for both the proton potential anomaly and the isobaric ( $p, n$ ) process.

(4) A surface-centered isospin potential<sup>24</sup> is able to produce a significantly better fit to the data for medium- $A$  nuclei than a pure volume term, indicating that there is some surface peaking of the isospin potential.

(5) It has been pointed out<sup>6,7</sup> that for targets of nonzero spin  $I$ ,  $V_1$  need not be a scalar and may contain even multipole moments of order  $l \leq 2I$ . Since there are no significant differences in the angular distributions for odd-even and even-even target nuclei, e.g.,  $\text{Fe}^{56}$  where  $I=0$  and  $\text{Mn}^{55}$  where  $I=\frac{5}{2}$ , one concludes that these data show no evidence for the existence of higher order multipole moments.

(6) Although the ratio of “quasi-inelastic” to “quasi-elastic” cross section for the medium- $A$  nucleus  $\text{Fe}^{56}$  is comparable to the ratio for the true mirror nucleus  $\text{B}^{11}$ , this ratio is more than an order of magnitude larger than calculations.<sup>7,24</sup>

In order to improve the ( $p, n$ ) data so that one may infer details of the isospin potential, the Livermore 90-in. cyclotron time-of-flight facility is presently being modified to provide better angular definition and better energy resolution.

## ACKNOWLEDGMENTS

It is a pleasure to acknowledge the assistance of D. R. Rawles and the 90-in. cyclotron crew in obtaining these data and of Dr. H. Mark for his comments regarding the interpretation of the data. We also wish to thank Dr. G. R. Satchler for making available several articles before publication and for many communications regarding the quasielastic ( $p, n$ ) reaction. The work was done under the auspices of the U. S. Atomic Energy Commission.